Adult-specific pheromones differently influence malthusian escape strategies of younger generations

Michael S. Werner[1,2], Marc H. Claaßen[1,2], Tess Renahan[1,2], Mohannad Dardiry[1], and Ralf. J. Sommer[1*]

[1]Department of Evolutionary Biology, Max Planck Institute for Developmental Biology, 72076 Tübingen, Germany

[2]These authors contributed equally

*Corresponding author: ralf.sommer@tuebingen.mpg.de

Abstract

Animals and plants can predict decreasing food supplies by recognition of population density, and respond by adjusting behavioral and morphological traits. Population density in nematodes is detected through pheromones, influencing dormant (dauer) stage entry, and in some lineages alternative mouth-form decision (bacterivorous vs. predatory). Whether age is a relevant parameter in recognizing population density is not well understood. Here, we utilized the mouth-form plasticity of the model nematode *Pristionchus pacificus* and developmental pheromone profiling to study potential parent:progeny communication. Surprisingly, we observed adult-specific production of molecules that induce the predatory morph, even though adult mouth forms are no longer plastic. We introduce a novel dye-based method to differentiate populations in mixed-generation cultures, and found adults, but not peers, influence developing juvenile mouth forms. Finally, we applied a logistic growth model that demonstrates adults both lower the population carrying capacity and decrease the time until resource depletion. In the necromenic life cycle of *P. pacificus*, we view mouth-form plasticity as an alternative 'Malthusian escape' strategy to dauer that responds to age-specific population densities.

Keywords: Pheromones, Phenotypic plasticity, Population density, *Pristionchus pacificus*, Nematode derived modular metabolites (NDMMs)

26 Population density is an important ecological parameter that correlates with increased
27 competition for resources[1]. In addition to density-dependent selection[2], which operates on
28 evolutionary time scales, some organisms can respond dynamically to population density by
29 phenotypic plasticity. For example, plants can sense crowding by detecting the ratio of red
30 (chlorophyll absorbing) to far red (non-absorbing) light, and respond by various shade-
31 avoidance strategies including higher shoots[3]. Locusts undergo solitary to swarm (i.e.
32 gregarious) transition, and aphids can develop wings, both as a result of increased physical
33 mechanosensory contact[4–6]. Intriguingly, population density can also have transgenerational
34 effects. For example, adult crowding of the desert locust *Schistocerca gregaria*[7,8] and migratory
35 locust *Locusta migratoria*[9] also influences the egg size, number, and morphology of their
36 progeny, and high population densities of red squirrels elicit hormonal regulation in mothers to
37 influence faster developing offspring[10]. Nevertheless, while incorporating age into population
38 structures has significantly advanced density-dependent selection theory[11], surprisingly little
39 age-specific refinement has been incorporated into models of phenotypic plasticity, especially at
40 the mechanistic level. This is partly due to the competing challenges of (1) studying population
41 ecology in the laboratory, and (2) the paucity of laboratory model organisms that are suitable for
42 ecological studies. The model nematode *Pristionchus pacificus* displays two types of phenotypic
43 plasticity that critically impact life history, developmental pathway and mouth form, providing an
44 experimentally tractable system to explore cross-generational influence[12,13].

45 In nematodes, high population densities induce entry into a stress resistant dormant
46 'dauer' stage (Fig. 1a), dramatically changing the population demographics. Many of the
47 molecular components that regulate dauer entry have been elucidated in both *Caenorhabditis*
48 *elegans*[14,15] and *P. pacificus*[16,17]. These studies point to a family of small molecule pheromones
49 called ascarosides that consist of an ascarylose sugar with a fatty acid side chain and modular
50 head and terminus groups[18–20](Fig. 1a). In *C. elegans* pheromones from all stages of
51 development can induce dauer[14], yet ascaroside production is sensitive to environmental cues

52 and increases with time[21]. In high population densities the major dauer-inducing ascaroside
53 exhibits a burst of production prior to dauer formation. Ascarosides also counteract another
54 currently unidentified crowding signal that stimulates growth rate in *C. elegans*[22], exemplifying a
55 common theme of density-dependent pheromone communication regulating life history traits in
56 nematodes. In *P. pacificus*, ascarosides also influence plasticity, although they are more
57 structurally diverse than in *C. elegans*[16,17,23,24]. For example, a parasotide-ascaroside derivative
58 influences dauer formation, and an ascaroside dimer influences the second type of plasticity in
59 *P. pacificus*, mouth form[16].

60 Adult *P. pacificus* exhibit either a narrow stenostomatous (St) mouth, which is restricted
61 to bacterial feeding (Figure 1b), or a wide eurystomatous (Eu) mouth with an extra denticle,
62 which allows for feeding on bacteria, fungi[25], and predation on other nematodes (Figure 1c)[26]. In
63 their natural habitat on a decaying beetle carcass (Fig. 1d), *P. pacificus* exits the dauer stage
64 and consumes microbial population blooms[13,27]. Animals with the St morph develop faster under
65 laboratory conditions on NGM agar plates[28]. If this holds true on the decaying beetle it may
66 provide a fitness benefit when microbes are abundant. However, it is predicted that bacterial
67 food will eventually become limiting in this isolated environment[27], and the Eu mouth form will be
68 advantageous to exploit additional food sources and remove competitors[29]. Presumably, second
69 or third generation juveniles can predict depleting resources by specifically sensing large
70 numbers of adults, triggering development of the Eu mouth form. However, the contribution of
71 age-structured populations to mouth form is unknown, and more broadly the role of age-
72 structured populations in phenotypic plasticity is poorly understood.

73 Here, we assess developmental regulation of ascaroside production in *P. pacificus* and
74 potential parent:progeny communication by preparing developmentally staged nematode
75 derived modular metabolite (NDMM) profiles from two natural isolates. Intriguingly, we observed
76 a binary switch of Eu-inducing NDMMs in adults. To test if this is physiologically significant, we
77 developed a novel multi-color dye method to differentiate between nematode populations,

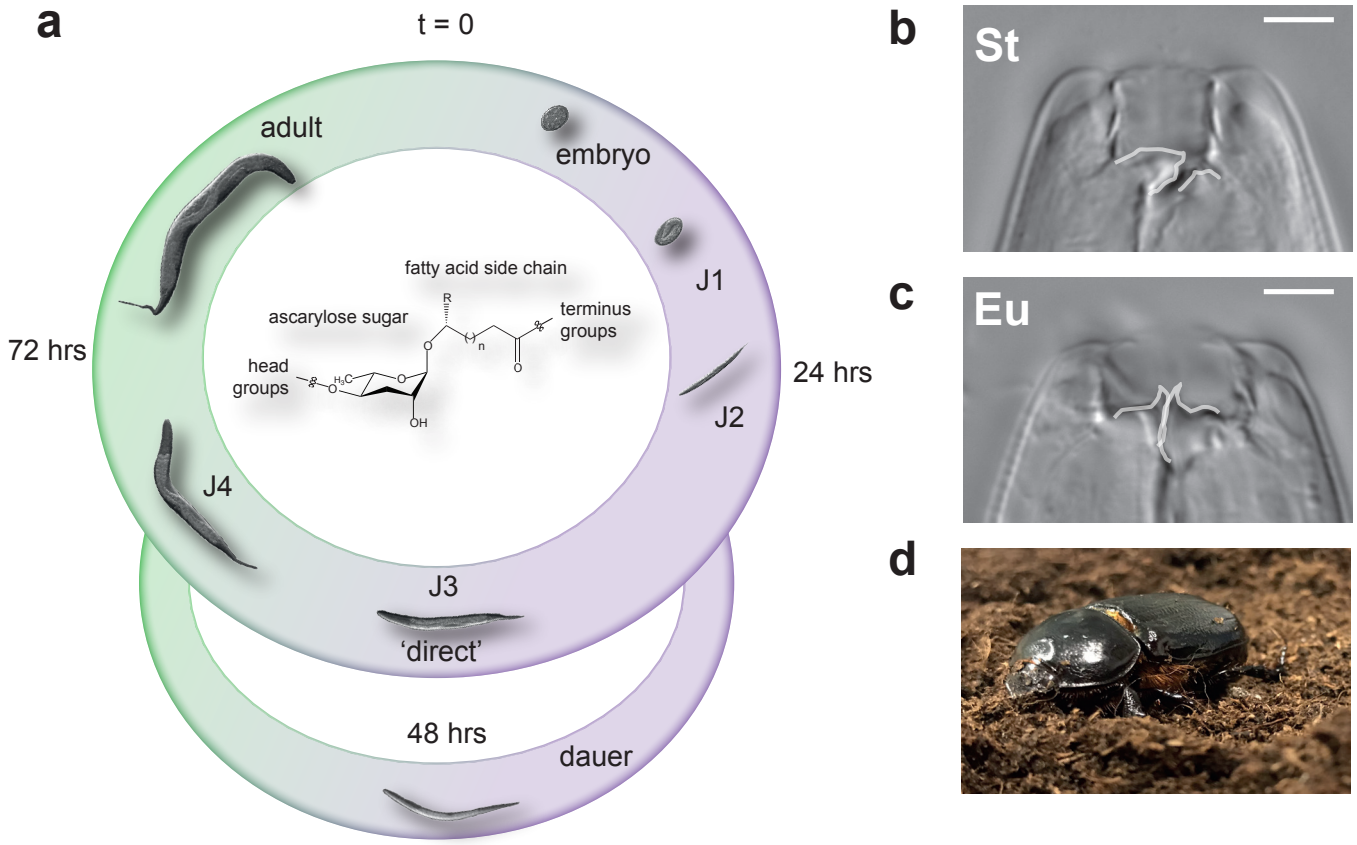

Fig. 1 | Life cycle and developmental plasticity of the model nematode *Pristionchus pacificus*. **a**, The life cycle of *P. pacificus* consists of four juvenile stages (J1-4) until sexual maturation (adults). Like many nematodes *P. pacificus* can enter a long-living 'dormant' dauer state that is resistant to harsh environmental conditions. The decision to continue through the 'direct' life cycle or enter dauer is regulated by small molecule excreted pheromones. **b**, *P. pacificus* can also adopt one of two possible feeding structures; either a microbivorous narrow-mouth (stenostomatous, St), or **c**, an omnivorous wide-mouth (eurystomatous, Eu) with an extra tooth that can be utilized to kill and eat other nematodes or fungi. White lines indicate the presence of an extra tooth (right side) in the Eu morph or its absence in the St morph, and the dorsal tooth (left side), which is flint-like in St and hook-like in Eu. White scale bar indicates 5 μM. **d**, *P. pacificus* typically exist in a necromenic association with beetles (shown here *Oryctes borbonicus*) in the dauer state, and re-enters the the feeding life cycle as J4s upon beetle death to feed on the ensuing microbial bloom.

allowing us to combine and observe different generations on the same plate. When juveniles were mixed with adults we observed a 10-20 fold induction of the Eu mouth form, while no effect was observed with similar numbers of mixed juveniles. Finally, we incorporated our experimental observations into a logistical growth model, which demonstrates a substantial reduction in time to reaching carrying capacity if adults are present. Thus, our data argue that age-specific population structure is a critical element of density-dependent phenotypic plasticity.

Results

In order to evaluate potential cross-generational communication in a nematode community we profiled *P. pacificus* pheromone levels in two strains through development. We used the laboratory strain RS2333 and the wild-isolate RSC017, and measured the exo-metabolomes of juvenile stage 2 (J2s, 24 hrs), J3s (48 hrs) and J4/adults (72 hrs) from a constant culture (Fig. 2a,b, Supplementary Fig. 1, Methods). Although the profiles were largely similar between strains, there were a few notable distinctions. The most striking being the abundance of Ubas compounds, a recently detected ascaroside dimer that has not been observed in other nematodes[16]. While Ubas#1 and #2 are prominent in RS2333, they are virtually nonexistent in RSC017, suggesting rapid allospecific evolution of NDMM production in *P. pacificus*, and evolution of conspecific regulation. Yet overall, both strains exhibited an increase over time of complex ascarosides, resulting in age-specific NDMM patterns (Fig. 2a,b). We were curious if this trend was due to a concomitant increase in body mass, however several observations suggest this is not the case. First, Pasc#9 and Pasc#12 exhibit a peak in abundance at the 48 hour/J3 time point, rather than in adults. Second, the overall area under the curve for each stage is between 8-36% of each other (Supplementary Fig. 1c), and third, the increase in NDMM abundance correlates with an increase in transcription of the thiolase *Ppa-daf-22.1*

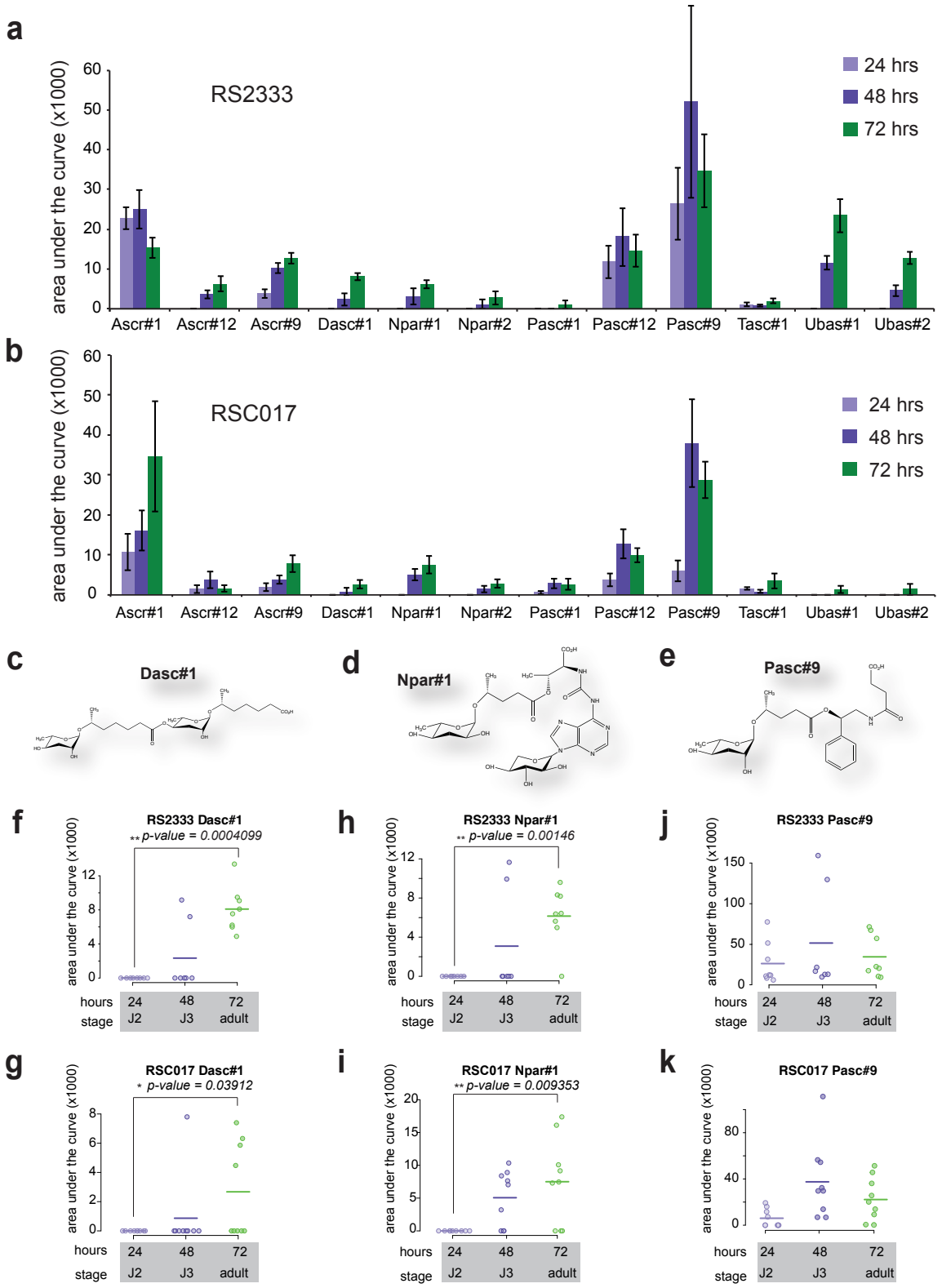

Fig. 2 | Time-resolved Nematode Derived Modular Metabolites (NDMMs) profile in *Pristionchus pacificus*. **a**, Time resolved secretion profile of nematode derived modular metabolites from the wild-type laboratory strain RS2333 and **b**, wild isolate RSC017. Data is presented as the mean of 8 (RS2333) and 9 (RSC017) biological replicates measured with two technical replicates, from 2 (RS2333) and 3 (RSC017) independent batches. **c-e**, Chemical structures of the Eu-inducing pheromone Dasc#1, the dauer and Eu-inducing pheromone Npar#1, and Pasc#9, a weak Eu-inducing pheromone, as described in the Small Molecule Identifier Database (http://www.smid-db.org/), produced in ChemDraw. **f-k**, Time-resolved abundance of Dasc#1, Npar#1, and Pasc#9 NDMMs in RS2333 and RSC017. Each data point represents a biological replicate, and bars represent mean abundance. P values calculated by two-sided Wilcoxon Rank Sum Test between 24 hr and 72 hr time points.

104 (Supplementary Fig. 2)[30], the most downstream enzyme in the β-oxidation pathway of
105 ascaroside synthesis[17]. Finally, we profiled the endo-metabolome of eggs, but find only
106 appreciable amounts of Asc#1,#9, #12, and Pasc#9, and little to no traces of the more complex
107 ascaroside derivatives (Supplementary Fig. 1d). Together, these findings suggest that many, if
108 not all, of the observed differences between stages correspond to age-specific production,
109 rather than a general correlation with body mass, or age-specific release.

110 Among the NDMMs that increase through development are Dasc#1, which is the major
111 Eu-inducing compound, and Npar#1, which is both Eu and dauer inducing[16] (Fig. 2c,d,f-i, $p <$
112 0.05 between adults and J2s, student's *t-test*). Closer inspection revealed that the trajectory of
113 Dasc#1 and Npar#1 production exhibits near binary kinetics, indicating switch-like induction
114 (Fig. 2f-i). In contrast, Pasc#9, which has only weak effects on mouth form or dauer[16], displays
115 more gradual fluctuations (Fig. 2e,j,k). These results suggest that the mode of induction is
116 NDMM specific, and that the kinetics of production may be related to their roles in phenotypic
117 plasticity. The observation that Dasc#1 and Npar#1 production switches on during the juvenile-
118 to-adult transition is especially intriguing because adults are no longer able to enter the dauer
119 phase or switch mouth forms, hinting at cross-generational signaling.

120 In order to measure cross-generational effects we first developed a novel dye-staining
121 methodology to differentiate between nematode populations. After trying several vital dyes we
122 identified that Neutral Red[31] and CellTracker Green BODIPY (Thermo) stain nematode
123 intestines brightly and specifically to their respective channels (Supplementary Fig. 3, Methods).
124 Importantly these dyes also stain *C. elegans* (Supplementary Fig. 4), dauers (Supplementary
125 Fig. 5), and last more than three days (Supplementary Fig. 6), allowing long term tracking of
126 mixed nematode populations. In contrast, nematodes exhibit high natural fluorescence in the
127 blue channel (i.e. DAPI), precluding the use of CellTracker Blue (Thermo) (Supplementary Fig.
128 2,3). Finally, neither Neutral Red nor CellTracker Green staining affect viability, developmental
129 rate, or mouth form (Supplementary Fig. 7).

130 To directly assess the effect of adults on juvenile populations we stained juveniles of the
131 highly St strain RSC017 (Fig. 3g) with Neutral Red, and added an increasing number of
132 CellTracker Green-stained adults or juveniles (Fig. 3f). Three days later we phenotyped red
133 adults that showed no green staining. Consistent with our chemical profiling, we observed a
134 significant (up to 48% Eu) density-dependent response to adults. In contrast, when juveniles
135 were raised with other juveniles, no significant change in Eu mouth form was detected (Fig.
136 3h,i). We were also curious if the thickened cuticle of dauers were still penetrable to
137 pheromones, allowing recognition of adults as they emerge from the dormant stage on the
138 decaying beetle carcass. Indeed, the same trend that was observed with juveniles was seen
139 with dauers, albeit to a more muted extent (Fig. 3j,k). With a total of 200 dauers and 500 adults
140 on one plate, 25.7% of dauers become Eu. In contrast, only 1.8% of dauers become Eu on a
141 plate containing 700 dauers (and no adults) (Fig. 3j). Collectively, these data demonstrate that,
142 at least in the context of our experimental set up, mouth-form plasticity is specifically induced by
143 adult crowding, whereas it is not affected by peer crowding.

144 Even though we did not detect a mouth-form switch in large populations of J2s or
145 dauers, and food was still visible on plates containing the most animals (500 adults and 200
146 juveniles), we could not totally rule out the possible effect of food availability on mouth form.
147 Therefore, we conducted assays with greatly increased numbers of juvenile competitors from
148 1,000 to 10,000, that would consume bacteria faster than in our previous assays. We noticed a
149 stark cliff in the fraction of juveniles that reach adulthood between 4,000-5,000 animals, arguing
150 that food is a limiting resource at this population density (Fig. 3l). Importantly however, in these
151 plates we still did not see a strong shift in mouth form. With an overwhelming 10,000 worms on
152 a plate, 5.8% were Eu, compared to 48% in the presence of only 500 adults. While food
153 availability may still have an impact during longer periods of starvation, under our experimental
154 conditions it appears to be negligible.

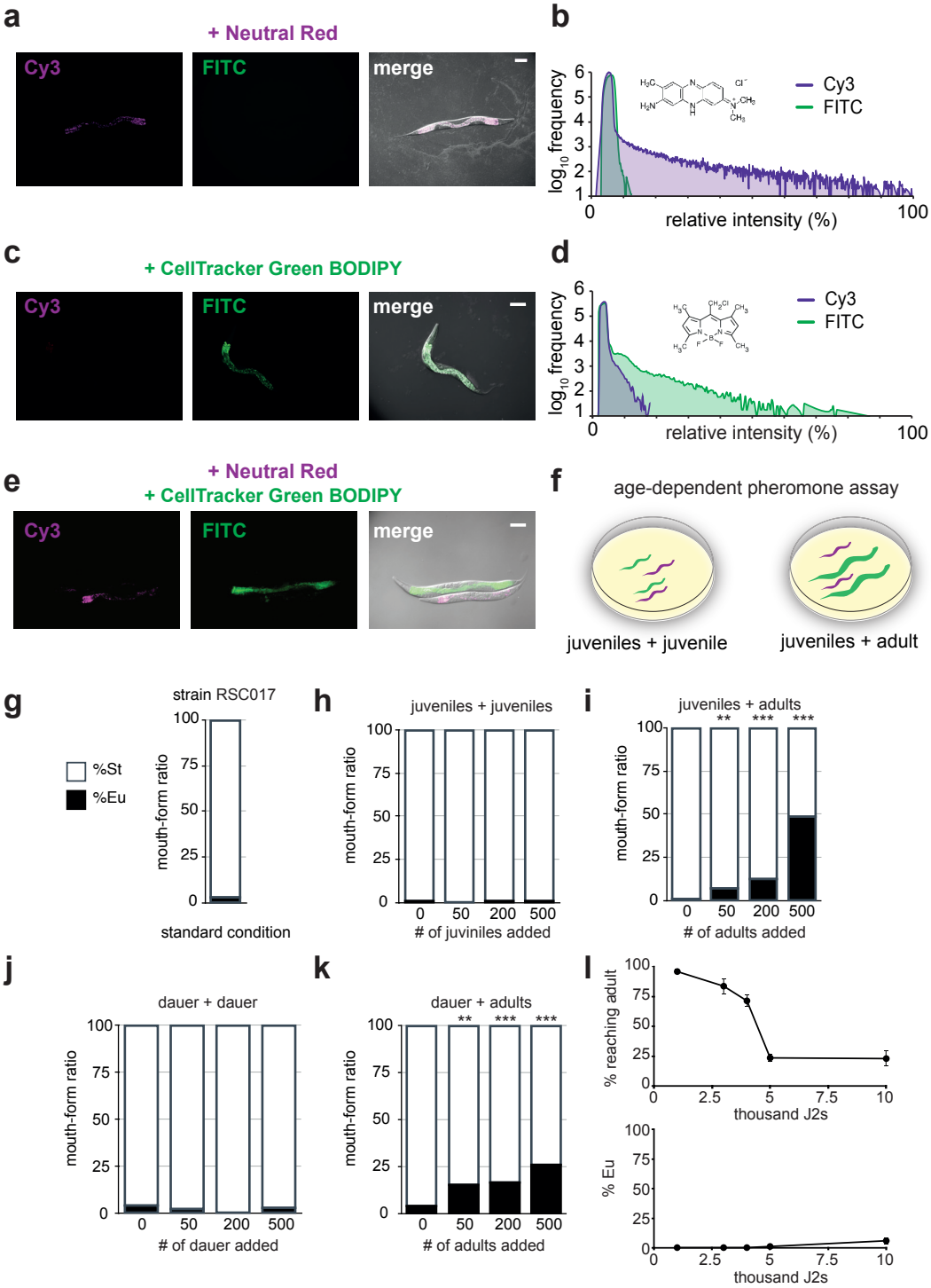

Fig. 3 | Adults influence the mouth form of juveniles. **a-e**, *P. pacificus* were stained with either 0.005% Neutral Red or 50 mM CellTracker Green Bodipy (Thermo) and viewed using Cy3 and FITC filters. Images were merged with Differential interference contrast (DIC), scale bar = 100 µM. The relative intensities of each fluorescence channel are displayed in the histograms (right) with the chemical structure of Neutral Red or CellTracker Green Bodipy. **f**, Age-dependent pheromone assay: Experimental juveniles were stained with Neutral Red, and challenged with CellTracker Green Bodipy-stained juveniles or adults on standard condition NGM agar plates seeded with 300 µl OP50 E. coli. Three days later, only red-positive and green-negative adults were phenotyped. **g**, The wild isolate RSC017 grown in standard conditions (5 young adults passed to fresh plates, progeny phenotyped 4 days later) are highly stenostomatous (<10%, n=102). **h-k**, When juveniles are raised with increasing number of peers they remain highly St (h), but when raised with adults (i) an Eu shift becomes apparent. This trend is also true when dauers are raised with other dauers (j) vs. adults (k). **l**, Percent reaching adulthood (top) and percent Eu of those that did reach adulthood (bottom) after increasing numbers of J2s are added to standard 6 cm NGM agar plates with bacteria (n=2 biological replicates).

155 The results from our chemical profiling and biological experiments demonstrate that
156 mouth form is exclusively sensitive to adult population density. This finding suggests that there
157 may be an ecological rationale for recognition of adults over peers. To formalize this rationale
158 we applied a logistic growth model that accounts for age-specific population structure and
159 phenotypic plasticity. Using empirically derived parameters, we modelled an exclusively juvenile
160 population vs. a population containing equal amounts of juveniles and adults (Methods, Fig. 4a).
161 Our model predicts two important effects when accounting for adults, (1) a 23% decrease in
162 carrying capacity (*K*=maximum population level), and (2) a decrease in time to reaching carrying
163 capacity from 6 to 10 days (1.7 fold difference, Fig. 4a, Methods). To verify the accuracy of our
164 model, which incorporates both food consumption and population increases, we conducted a
165 feeding assay for 18 and 72 hours. The 18 hour time frame only reflects consumptive
166 differences, while the 72 hour time frame also allows the progeny from adults to develop into
167 feeding larval stages, thereby also accounting for an increase in population size. After 72 hours
168 we observed a 2.6 ± 1.6 fold difference in remaining bacterial food (Fig. 4b), which falls within
169 our model's predictive difference of 1.7.

170 As we demonstrated above, juveniles respond to increasing adult population densities
171 by inducing the Eu morph. In our experimental assays (Fig. 3), induction occurred as early as 50
172 adults (250 total individuals), and reached nearly 50% Eu with the addition of 500 adults (700
173 total individuals). Consistent with our expectation that the Eu morph is an ecological response
174 strategy, population growth becomes logarithmic in this size regime (Fig. 4b), leaving only 2-3
175 days until reaching carrying capacity *K*. Theoretically, inducing the Eu morph should correspond
176 to an increase in *K*, so we conservatively modelled a 1.5-fold effect (upper grey line, Fig. 4a),
177 which leads to an increase from six days to seven days to reach *K* (Supplementary Fig. 8).
178 Importantly, this is still within the egg-laying period[32], potentially contributing to increased
179 fitness. Nevertheless, these assumptions are subject to several difficult-to-measure factors that
180 could both positively and negatively affect *K*, such as the consumption rate of other nematode

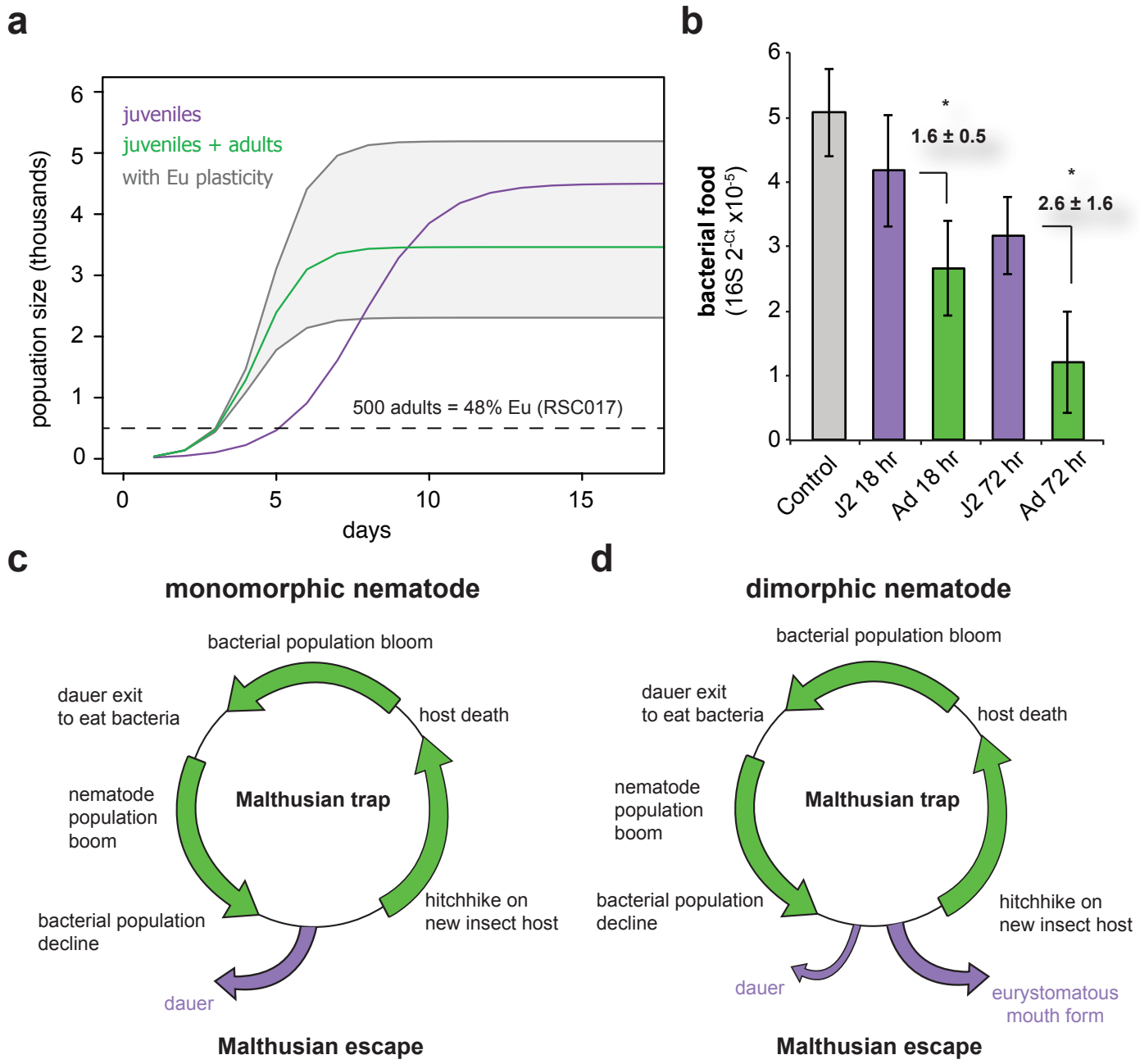

Fig. 4 | Logistic growth model of age-structured populations indicates ecological rationale for adult-specific influence on mouth form. **a**, Logistic growth model with empirically derived parameters (see Methods) for juvenile only populations (purple), juvenile:adult populations (green), and juvenile:adult populations that can switch to the Eu morph (grey). The wide-range of possible outcomes when incorporating the Eu morph is based on a conservative estimates that could positively or negatively influence the carrying capacity (K). Dashed line indicates the population size at which we previously observed a strong shift in Eu frequency (Fig. 3). **b**, Remaining *E.coli* food after 0 (control), 18 hr, and 72 hrs, measured by quantitative PCR (qPCR) with universal 16S primers 906 F and 1062 R. **c**, Conceptual life cycle models of monomorphic or **d**, dimorphic mouth form nematodes that exist in necromenic association with insect hosts. At some point in the isolated niche of the decaying carcass, microbial food supplies will run out, leading to a Malthusian catastrophe. Nematodes temporarily escape this trap by entering the dauer state, hitchhiking to a new insect carrier, and re-starting the cycle. Dimorphic nematodes can sense the impending catastrophe earlier by recognizing an abundance of adults in the population, switching to the Eu morph, and exploiting new resources. By analogy to economic models, dauer and mouth form are technological innovations to escape resource traps.

181 populations, the nutritional value of different food sources, and the removal of competitors by
182 predation. Hence, we also estimate a wide-range of possible scenarios by tuning *K* (±1.5 fold,
183 grey lines, Fig. 4b). Depending on the stochasticity of the aforementioned factors, we suspect
184 that in nature the actual *K* and time to reaching *K* will fall somewhere within this range. In
185 summary, our model estimates a quantitative impact of accounting for adults that reflects
186 empirical data, which can be offset by inducing the Eu mouth form. The broader implications of
187 these findings relative to phenotypic plasticity and density dependence are further considered in
188 the Discussion.
189
190
191 **Discussion**
192
193 *P. pacificus* recognizes population density by pheromone detection, which can influence
194 developmental decisions including dauer entry and mouth form. Here, we present the first
195 developmental time series of pheromones in *P. pacificus*, which i) show an age-dependent
196 increase in NDMMs that affect life history and mouth-form plasticity, ii) exhibit a surprising 'off-
197 on' induction pattern unknown in the literature, iii) developed a novel dye-based method that
198 allowed us to determine cross-generational influence on mouth form, and iv) incorporated age
199 and mouth-form plasticity into a population growth model to account for our observations.
200 Collectively, our results argue that age-structured populations should be incorporated into
201 descriptions of density-dependent phenotypic plasticity.
202 Our developmental profiling of pheromones revealed an overall trend of increased
203 production of complex NDMMs over time. The observation that this trend mirrors the
204 transcriptional regulation of enzymes involved in NDMM synthesis argues that the stage-
205 dependent increase is not merely a result of an increase in body mass, but rather that these
206 molecules are programmed for stage-specific induction. The binary 'on-off' kinetics observed for

207 some NDMMs might reflect a population level feed-back loop, such that the production of
208 density-sensing pheromones is based on a threshold level of previously produced pheromones.

209 Among the many environmental influences on mouth form[33], population density and
210 starvation is perhaps the most ecologically relevant. Indeed they have been shown to affect
211 numerous *P. pacificus* strains[16,34], but teasing apart these two factors has proven difficult. Here
212 we demonstrate that while a strong shift is observed with adult specific pheromones, no such
213 effect was seen under limited resource conditions. Thus, in a short time frame, age-specific
214 crowding is the major environmental factor. However, this does not preclude that long term
215 starvation could also have an effect.

216 Although Npar#1 is also a major dauer inducing pheromone in *P. pacificus*, we observed
217 no increase in the amount of dauers in either adult or juvenile plates. Thus, it seems that mouth-
218 form phenotype is the major plastic response to adult populations, at least at the densities used
219 in our experiment. Presumably higher concentrations are required for dauer induction, reflecting
220 a calculated response strategy depending on the level of crowding.

221 Given that St animals develop faster[28], there may be a 'race' to sexual maturation in
222 emergent populations. Yet as the nematode population increases on the isolated niche of the
223 decaying beetle carcass, there will likely be a commensurate decrease in bacterial populations.
224 At some point the adaptive advantage would switch from the St to Eu morph, and then
225 ultimately dauer entry. In this context, by analogy to economic models of population growth[35,36],
226 we view mouth-form plasticity and dauer formation as alternative 'technological innovations' to
227 escape a 'Malthusian resource trap' (Fig. 4c-d). When population densities of monomorphic-
228 mouth form nematodes, such as *C. elegans*, reach the carrying capacity they enter the dauer
229 stage and disperse, re-starting the cycle. However, dimorphic species like *P. pacificus* have
230 evolved an alternative strategy that senses population densities of adults. When nematode prey
231 is the only available food source, the Eu morph provides longer life spans leading to more
232 progeny[29], and presumably increased fitness. Going forward, the challenge will be to test these

233 relationships and predictions in more natural simulated environments with increasing complexity
234 of variables. Finally, whether cross-generational communication reflects an intended signal from
235 adult to juveniles, i.e. kin selection[37], or more simply, evolved recognition by juveniles of adult-
236 produced pheromones, is a tantalizing question for subsequent research. But regardless of
237 those interpretations, our results demonstrate that in the future age-structured populations
238 should be incorporated into the theory of phenotypic plasticity.
239
240
241 **Methods**
242
243 **Nematode strains and husbandry**
244 *P. pacificus* Wild-type RS2333 (California) and RSC017 (La Réunion) strains were kept on 6 cm
245 nematode growth media (NGM) plates seeded with OP50 and kept at 20°C. RSC017 is highly
246 St and does not predate on other nematodes, and thus was used for biological assays instead
247 of the highly Eu, predatory RS2333.
248
249 **Pheromone profiling**
250 **HPLC-MS sample preparation for normal exo-metabolome and time resolved analysis**
251 To collect staged phermone profiles, we seeded 35 x 6 cm plates with 5 worms each, and
252 bleached 5-6 days later when gravid to collect eggs/J1s. These were then seeded in 6 x 10 mL
253 flasks with OP50 as described in Werner et al., 2017[33]. Then at 24, 48, or 72 hr time intervals,
254 supernatant was obtained by centriguation (>4,000 x g, 4°C for 10 minutes). 1 mL supernatant
255 was adsorbed onto a SPE-C8 cartridge (Thermo Scinetific Hypersept C8 100 mg/1mL),
256 conditioned with 1 mL MeOH followed by 2 mL Millipore water. The adsorbed material was then
257 washed with 200 uL water and subsequently eluted with 200 uL MeOH. This extract was then
258 measured directly via HPLC-qTof MS (Bruker ImpactII).

259

260 **HPLC-MS measurement**

261 20 uL extract was injected into a Thermo ultimate 3000 HPLC equipped with a Sigma-Alderich
262 Ascentis Express C18 2.7um 10mm x 4.6mm column at 20 °C with a flow of 500 uL/min. All MS
263 measurements have been performed in negative ion mode and molecules are detected as [M-
264 H]$^-$ Ions. The solvent gradient started with 5 % acetonitrile (ACN)/ 95 % water (both containing
265 0.1 % formic acid) for 2 min. After this equilibration step, the ACN proportion has been
266 increased to 65 % over 8 min, then to 100 % ACN in 1.2 min followed by a hold step for 8.8 min.
267 Afterwards, they system was flushed to 5 % ACN with 2 min equilibration for a total of 22 min.
268 For calibration, a sodium formiat cluster building solution has been automatically injected in the
269 first 2 minutes of each run.

270

271 Data analysis was performed with TASQ version 1.0 from Bruker Daltonics. Therefore,
272 extracted ion chromatograms for each well-known compound with a mass wide of 0.1 m/z and
273 time slices of 0.5 min around the expected retention time has been produced after calibrating
274 and baseline correction. Assignment errors have been corrected with the provided MRSQ value.

275

276 **Dye staining**

277 A stock solution of Neutral Red was prepared by dissolving 0.5 mg in 10 ml 5% acetic acid and
278 stored at -20° C. Working solutions were prepared by 100x dilution in M9, aliquoted, stored at -
279 20°C, and thawed directly before use. Working solutions were kept for approximately 1 month
280 before re-making. J2s were prepared from 20-40 6cm plates 6 days after passaging 5 worms to
281 each plate on 300 µl OP50. Worms were washed from plates with M9 into a conical tube, and
282 then filtered through 2x20 µM filters (Millipore) placed between rubber gaskets. The flow-
283 through contains mostly J2 and some J3, which were pelleted by centrifugation, 8 seconds on a
284 table-top eppdendorf centrifuge 5424, reaching approximately 10,000 x g. The juvenile pellet

285 was then either re-suspended in 1 ml Neutral Red working solution, or in 1 ml M9 and split to
286 two tubes, then re-centrifuged, and then re-suspended in either 1 ml working solution Neutral
287 Red (0.005% in M9) or 1 ml 50 µM Green BODIPY (Thermo) in M9. Tubes were then rotated for
288 3 hours in the dark, then washed by centrifugation as before, and re-suspended in 1 ml M9. This
289 was repeated 3-4x until the dye was no longer visible. Then the concentration of worms were
290 determined by aliquoting 2 µl onto a glass coverslip in 5 technical replicates, and counted under
291 a dissecting microscope. Finally the appropriate number of animals was added to 6 cm plates
292 that had been previously seeded with 300 µl OP50, then incubated at 20°C. After 3 days, 100%
293 of worms exhibited Neutral Red staining (*n*=50, Supplementary Fig. 6,7). Dauers and J2s
294 recovered after Neutral Red staining developed at the same developmental speed (3-4 days)
295 and with the same mouth-form ratio as control worms recovered side-by-side (100% St for both,
296 Supplementary Fig. 7, *n*=30). Dauers and J2s stained with Cell tracker Green BODIPY (50 µM)
297 (Thermo) were similar, although slightly less effeciently stained compared to Neutral Red. After
298 three days 90% retained intestinal fluorescence, although brightness decreased with the
299 number of days. Mouth-form ratios of dauers or J2s in +/- 50 µM Cell tracker Green BODIPY
300 developed at equivalent rates and mouth-form ratios. Lower than 25 µM did not yield strongly
301 fluorescent worms after three hours. Cell Tracker Blue CMAC (Thermo) was also used at 50 µM
302 and imaged 3 days post-staining for *P. pacificus*, and one day post-staining for *C. elegans*.
303 However, due to the higher fluorescent background in the blue light spectrum in both *P.*
304 *pacificus* and *C. elegans*, we performed all experiments using only Neutral Red and Cell tracker
305 Green BODIPY.
306
307 **Microscopy**
308 All images were taken on a Zeiss Axio Imager 2 with an Axiocam 506 mono, and processed
309 using Zen2 pro software. Image brightness and contrast were enhanced in ImageJ with a

310 minimum displayed value of 10 and maximum of 100 for all images in Fig 3, and Supplementary
311 Fig. 3 and 4, and a minimum of 21 and maximum of 117 for Supplementary Fig. 5.
312
313 The following exposure times were used for all images:
314 Cy3 (peak emission = 561, exposure = 80 ms), FITC (peak emission = 519, exposure = 150
315 ms), Dapi (peak emission = 465, exposure = 80 ms), DIC (exposure = 80-140 ms).
316
317 **Dauer induction**
318 To induce dauer, mixed-stage plates with little to no OP50 were washed with M9 and the
319 resulting worm pellets were used in a modified 'White Trap' method. Worm pellets were placed
320 on killed *Tenebrio molitor* grubs and dispersing dauers were collected in surrounding MilliQ
321 water. Age of dauers ranged from one week to one month.
322
323 **Logistic Model**
324 We applied the analytic solution (equation 2) to the logistic growth/Verhulst-Pearl[38] (equation 1):
325
326 (1)

$$P(t) = r \cdot P(1 - \frac{P}{K})$$

327
328 (2)

$$P(t) = \frac{K}{1 + \left(\frac{K}{P(0)} - 1\right) \cdot e^{rt}}$$

329
330 where:
331 *P(t)* = Population size as a function of time

332 *K* = Carrying capacity (maximum sustainable population)

333 *P(0)* = Initial population size, estimated at 10 animals from previous field studies (Meyer et al.,

334 2017[27] and T. Renahan, personal communication).

335 *t* = Time (days)

336 *e* = *eulers* number = 2.71828

337 *r* = Intrinsic growth rate (also known as r_{max})

338

339 For carrying capacity (*K*), we estimated 4,500 animals, based on our previous experiment that

340 identified the number of animals that can reach adulthood prior to starvation (on 6 cm agar

341 plates with 300 µl OP50 *E. coli*, Fig. 3I). To account for adults, we first collected data to input

342 into our model. Intuitively, we hypothesized that adults may consume more bacteria than

343 juveniles, thus depleting food sources faster. After 18 hours of *ab libitum* feeding on *E. coli*, we

344 observed 1.6 ± 0.5 fold more bacteria consumed by adults compared to juveniles (qPCR of 16S,

345 Fig. 4b). Importantly, at this time point any progeny produced by adults has not yet hatched

346 (<24 hours), so this measurement is purely based on the consumptive differences. We used

347 this 1.6 factor to compute a carrying capacity when accounting for an equal population of adults

348 and juveniles (i.e. 1.3), so $K_{J2:adults}$= 4,500 ÷1.3 = 3,461.5. We then calculated an intrinsic growth

349 rate (*r*) using previously published life history data (Supplementary Table 1)[32,39]. For a

350 theoretical ½ adult, ½ juvenile population (green line, Fig. 4a) we made an '½ adult' table by

351 adjusting the first few rows 'up' to begin reproduction and egg deposition at day 1, without the

352 normal 3-day lag period, and adjusted fecundity and the number of animals (N_x) by 0.5x. These

353 values were then added to a 0.5x juvenile population (Supplementary Table 1). We then

354 calculated an intrinsic growth rate (*r*) for a juvenile-only population, or juvenile:adults (r_a) using

355 iterative calculations of Euler's[40] equation (equation 3):

356

357 (3)

$$\sum_{x=0}^{d} e^{-rt} \cdot lx \cdot mx = 1$$

358

359 Where:

360 *lx* = age-specific survival = $N(t) \div N_{start}$

361 *mx* = age-specific fecundity = fecundity $f(t) \div N(t)$

362 **N* = number of animals

363

364 To account for the Eu mouth form, we modelled that the ability to eat fungi or prey on other
365 nematodes would affect the overall carrying capacity. However, we did not feel that we could
366 estimate a reliable numerical value because of the myriad extrinsic factors that could occur in
367 nature (consumption rate of other nematode populations, nutritional value of nematodes or
368 fungi, the effect of reducing competitors by predation, etc.), so we simply calculated
369 conservative upper and lower bounds of K_a (by a factor of 1.5 in either direction), and plotted the
370 resulting growth models (grey lines). To find the time to reaching carrying capacity, we
371 calculated the minium (t) of the 2nd derivitive of equation 2 for each population (Supplementary
372 Fig. 8).

373

374

375 **Author Contributions**

376 MSW and RJS conceived of the project. MC designed and conducted pheromone profiling, TR
377 and MSW designed and conducted all biological experiments. MD, TR, and MSW performed
378 ecological modeling. MSW and TR wrote the manuscript with input and edits from all authors.

379

Acknowledgements

We would like to thank all members of the Sommer lab, and Dr. Cameron Weadick (University of Sussex), Justin Lewis (University of Florida), and Dr. Talia Karasov (Max Planck Institute) for their thoughtful critique and discussion.

References

1. Hastings, A. *Population Biology: Concepts and Models*. (Springer Science & Business Media, 1997).
2. Macarthur, R. H. Some Generalized Theorems of Natural Selection. *Proc. Natl. Acad. Sci. U. S. A.* **48,** 1893–1897 (1962).
3. Casal, J. J. & Smith, H. The function, action and adaptive significance of phytochrome in light-grown plants. *Plant Cell Environ.* **12,** 855–862 (1989).
4. Pener, M. P. & Simpson, S. J. Locust Phase Polyphenism: An Update. in *Advances in Insect Physiology* (eds. Simpson, S. J. & Pener, M. P.) **36,** 1–272 (Academic Press, 2009).
5. Sloggett John, J. & Weisser Wolfgang, W. A general mechanism for predator-and parasitoid-induced dispersal in the pea aphid, Acyrthosiphon pisum. *Aphids in a New Millennium* 79 (2004).
6. Simpson, S. J., Despland, E., Hägele, B. F. & Dodgson, T. Gregarious behavior in desert locusts is evoked by touching their back legs. *Proc. Natl. Acad. Sci. U. S. A.* **98,** 3895–3897 (2001).
7. Hunter-Jones, P. Laboratory studies on the inheritance of phase characters in locusts. *Anti-Locust Bulletin* 1–32 (1958).
8. Maeno, K. & Tanaka, S. Maternal effects on progeny size, number and body color in the desert locust, Schistocerca gregaria: Density- and reproductive cycle-dependent variation. *J. Insect Physiol.* **54,** 1072–1080 (2008).
9. Chen, B. *et al.* Paternal epigenetic effects of population density on locust phase-related characteristics associated with heat-shock protein expression. *Mol. Ecol.* **24,** 851–862 (2015).
10. Dantzer, B. *et al.* Density triggers maternal hormones that increase adaptive offspring growth in a wild mammal. *Science* **340,** 1215–1217 (2013).

11. Charlesworth, B. *Evolution in Age-Structured Populations*. (Cambridge University Press, 1994).
12. Viney, M. & Harvey, S. Reimagining pheromone signalling in the model nematode Caenorhabditis elegans. *PLoS Genet.* **13,** e1007046 (2017).
13. Sommer, R. J. & McGaughran, A. The nematode Pristionchus pacificus as a model system for integrative studies in evolutionary biology. *Mol. Ecol.* **22,** 2380–2393 (2013).
14. Golden, J. W. & Riddle, D. L. A pheromone influences larval development in the nematode Caenorhabditis elegans. *Science* **218,** 578–580 (1982).
15. Butcher, R. A., Fujita, M., Schroeder, F. C. & Clardy, J. Small-molecule pheromones that control dauer development in Caenorhabditis elegans. *Nat. Chem. Biol.* **3,** 420–422 (2007).
16. Bose, N. *et al.* Complex small-molecule architectures regulate phenotypic plasticity in a nematode. *Angew. Chem. Int. Ed Engl.* **51,** 12438–12443 (2012).
17. Markov, G. V. *et al.* Functional Conservation and Divergence of daf-22 Paralogs in Pristionchus pacificus Dauer Development. *Mol. Biol. Evol.* **33,** 2506–2514 (2016).
18. Choe, A. *et al.* Ascaroside signaling is widely conserved among nematodes. *Curr. Biol.* **22,** 772–780 (2012).
19. Srinivasan, J. *et al.* A modular library of small molecule signals regulates social behaviors in Caenorhabditis elegans. *PLoS Biol.* **10,** e1001237 (2012).
20. Butcher, R. A. Small-molecule pheromones and hormones controlling nematode development. *Nat. Chem. Biol.* **13,** 577–586 (2017).
21. Kaplan, F. *et al.* Ascaroside expression in Caenorhabditis elegans is strongly dependent on diet and developmental stage. *PLoS One* **6,** e17804 (2011).
22. Ludewig, A. H. *et al.* Larval crowding accelerates C. elegans development and reduces lifespan. *PLoS Genet.* **13,** e1006717 (2017).
23. Bose, N. *et al.* Natural variation in dauer pheromone production and sensing supports intraspecific competition in nematodes. *Curr. Biol.* **24,** 1536–1541 (2014).

24. Yim, J. J., Bose, N., Meyer, J. M., Sommer, R. J. & Schroeder, F. C. Nematode signaling molecules derived from multimodular assembly of primary metabolic building blocks. *Org. Lett.* **17,** 1648–1651 (2015).

25. Sanghvi, G. V. *et al.* Life History Responses and Gene Expression Profiles of the Nematode Pristionchus pacificus Cultured on Cryptococcus Yeasts. *PLoS One* **11,** e0164881 (2016).

26. Wilecki, M., Lightfoot, J. W., Susoy, V. & Sommer, R. J. Predatory feeding behaviour in Pristionchus nematodes is dependent on phenotypic plasticity and induced by serotonin. *J. Exp. Biol.* **218,** 1306–1313 (2015).

27. Meyer, J. M. *et al.* Succession and dynamics of Pristionchus nematodes and their microbiome during decomposition of Oryctes borbonicus on La Réunion Island. *Environ. Microbiol.* **19,** 1476–1489 (2017).

28. Serobyan, V., Ragsdale, E. J., Müller, M. R. & Sommer, R. J. Feeding plasticity in the nematode Pristionchus pacificus is influenced by sex and social context and is linked to developmental speed. *Evol. Dev.* **15,** 161–170 (2013).

29. Serobyan, V., Ragsdale, E. J. & Sommer, R. J. Adaptive value of a predatory mouth-form in a dimorphic nematode. *Proc. Biol. Sci.* **281,** 20141334 (2014).

30. Baskaran, Praveen, *et al*. Ancient gene duplications have shaped developmental stage-specific expression in Pristionchus pacificus. *BMC evolutionary biology* **15.1**, 185 (2015).

31. Thomas, M. C. & Lana, P. da C. Evaluation of vital stains for free-living marine nematodes. *Brazil. J. Oceanogr.* **56,** 249–251 (2008).

32. Gilarte, P., Kreuzinger-Janik, B., Majdi, N. & Traunspurger, W. Life-History Traits of the Model Organism Pristionchus pacificus Recorded Using the Hanging Drop Method: Comparison with Caenorhabditis elegans. *PLoS One* **10,** e0134105 (2015).

33. Werner, M. S. *et al.* Environmental influence on Pristionchus pacificus mouth form through different culture methods. *Sci. Rep.* **7,** 7207 (2017).

34. Bento, G., Ogawa, A. & Sommer, R. J. Co-option of the hormone-signalling module dafachronic acid–DAF-12 in nematode evolution. *Nature* **466,** 494 (2010).

35. Malthus, T. R. An Essay on the Principle of Population. Reprint 2004. Edited with an introduction and notes by Geoffrey Gilbert. (1798).

36. Trewavas, A. Malthus foiled again and again. *Nature* **418,** 668–670 (2002).

37. Bourke, A. F. G. Hamilton's rule and the causes of social evolution. *Philos. Trans. R. Soc. Lond. B Biol. Sci.* **369,** 20130362 (2014).

38. Verhulst, P. F. Recherches Mathématiques sur La Loi D'Accroissement de la Population, Nouveaux Mémoires de l'Académie Royale des Sciences et Belles-Lettres de Bruxelles, 18, Art. 1, 1-45. (1845).

39. Weadick, C. J. & Sommer, R. J. Mating System Transitions Drive Life Span Evolution in Pristionchus Nematodes. *Am. Nat.* **187,** 517–531 (2016).

40. Lotka, AJ. *Elements of Physical Biology*. (Williams & Wilkins, 1925).

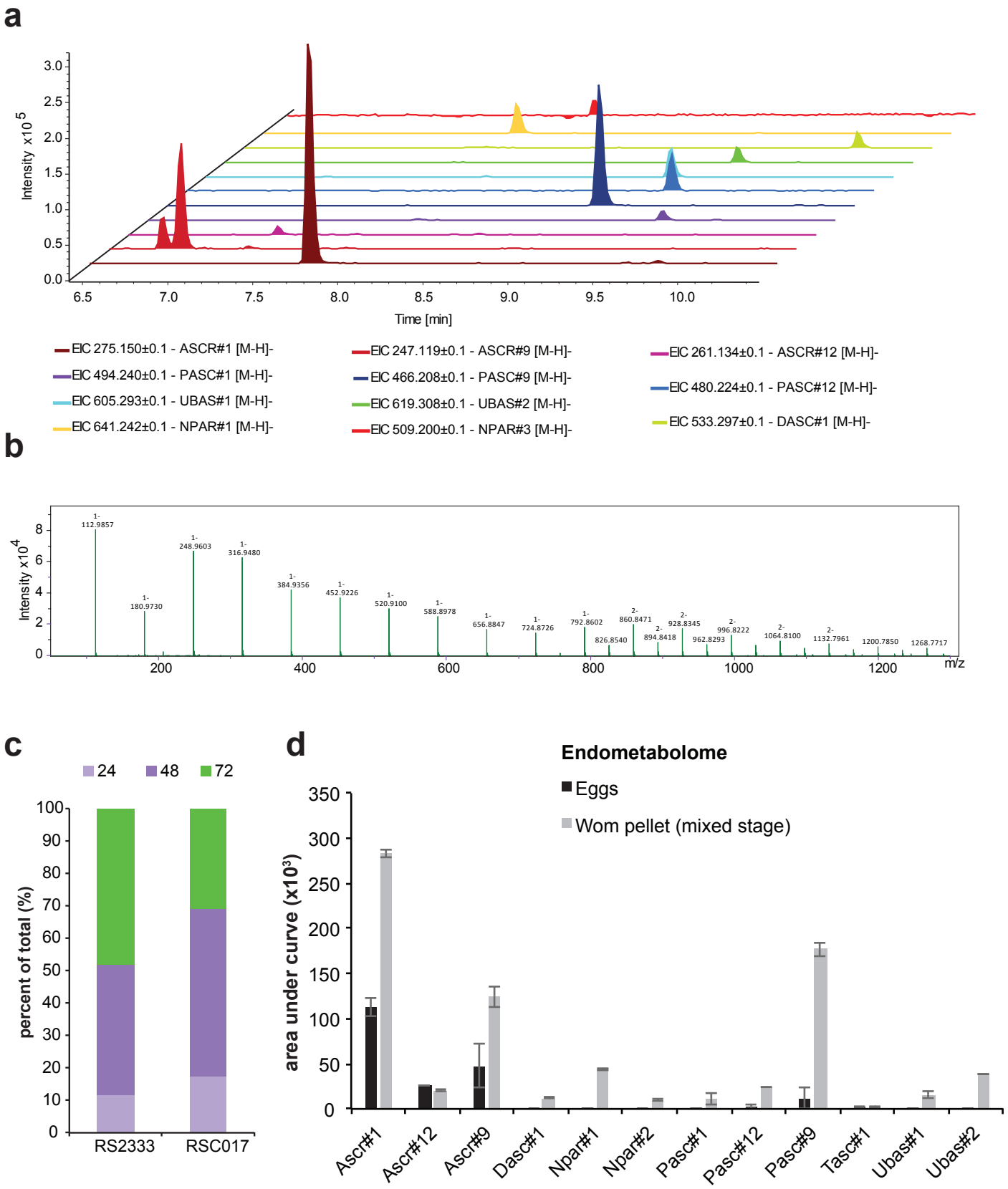

Supplementary Figure 1 | Pheromone profiling quality control. a, Extracted ion traces (width 0.1 m/z) of the NDMM used in this publication from a sevens day mixed-stage sample, double peak of 247.12 m/z indicate isomeric structures (Part#9/Ascr#9). **b**, Example of an averaged spectrum over a calibration segment, sodium-formiat cluster building solution has been used to ensure high mass accuracy in each run. **c**, Percent abundance of NDMMs per time point from both strains. **d**, Comparison of an endometabolome sample from a seven day mixed-stage cultured compared to the endometabolome of eggs, produced by using bleached eggs from 80 x 60 mm plates.

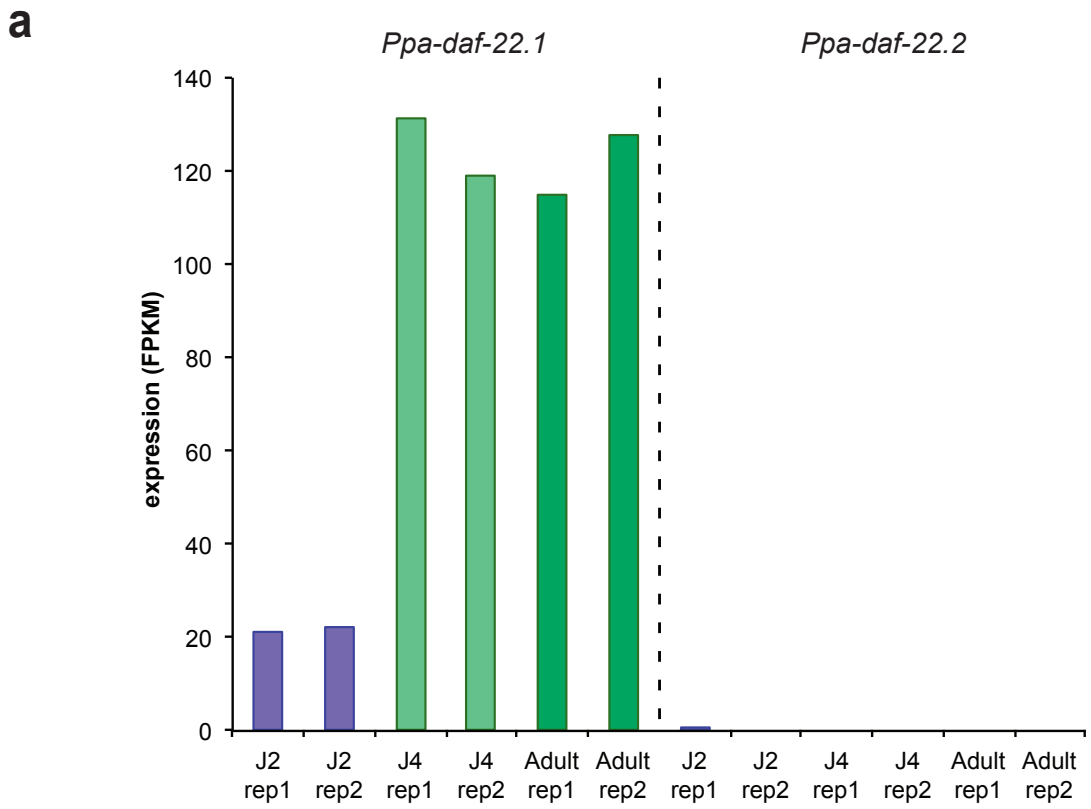

Supplementary Figure 2 | Enzyme that synthesize NDMMs is transcriptionally regulated during development.

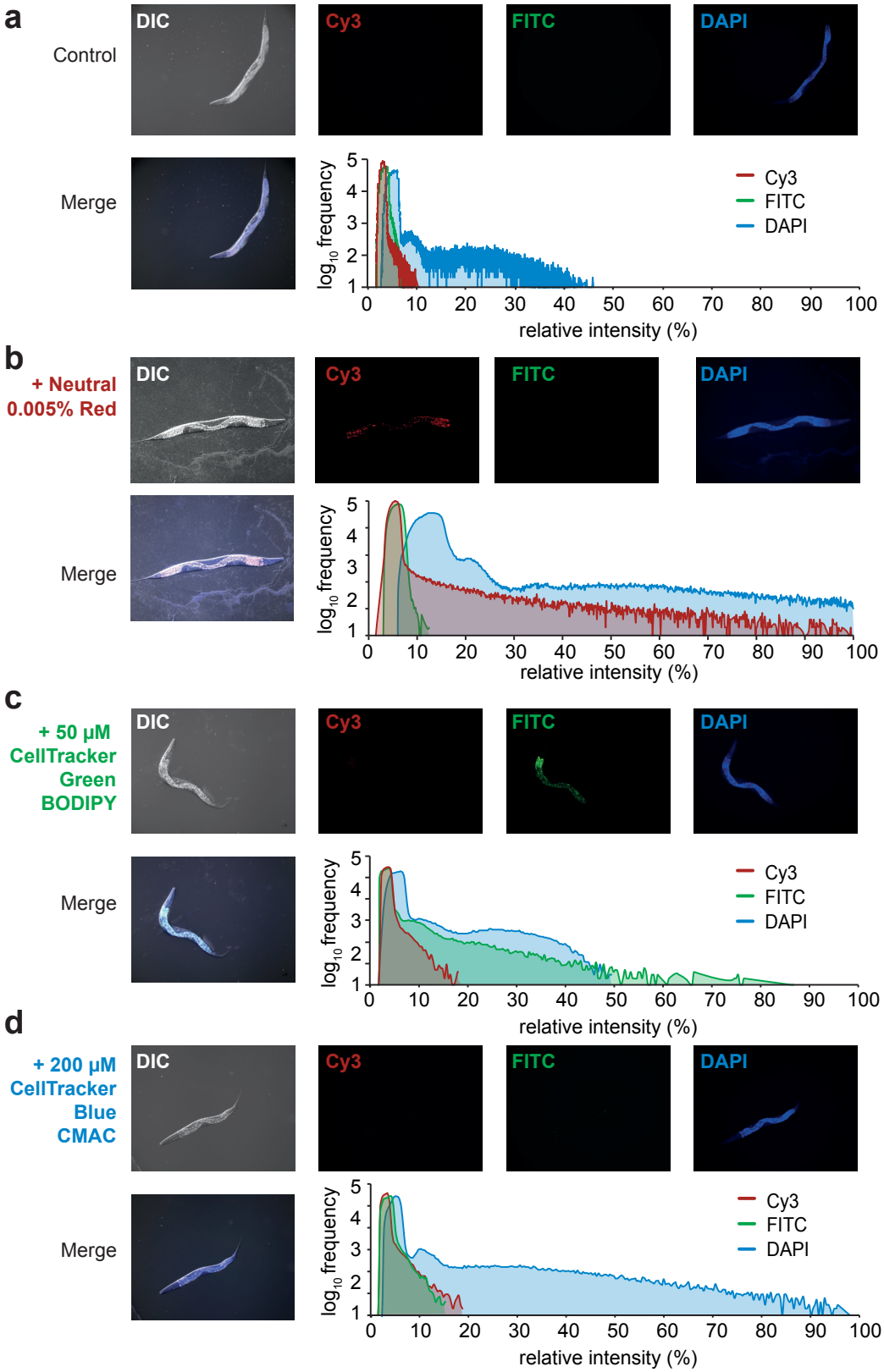

Supplementary Figure 3 | Vital dye staining of *Pristionchus pacificus*. **a**, Control *P. pacificus* imaged with Cy3, FITC, and DAPI filters, and a merge with Differential Interference Contrast (DIC). Histogram on the right represents quantification of intensity with each filter. **b**, Same as **a**, but stained with 0.005% Neutral Red, **c**, 50 µM CellTracker Green Bodipy (Thermo Fischer), or **d**, CellTracker Blue CMAC Dye (Thermo Fischer). J2s were stained (methods), and ensuing adult animals were imaged 3 days later on a Zeiss Axio Imager 2 with an Axiocam 506 mono, and processed using Zen2 pro software. Image brightness and contrast were enhanced in ImageJ for display, with a minimum displayed value of 10 and maximum of 100 for all images.

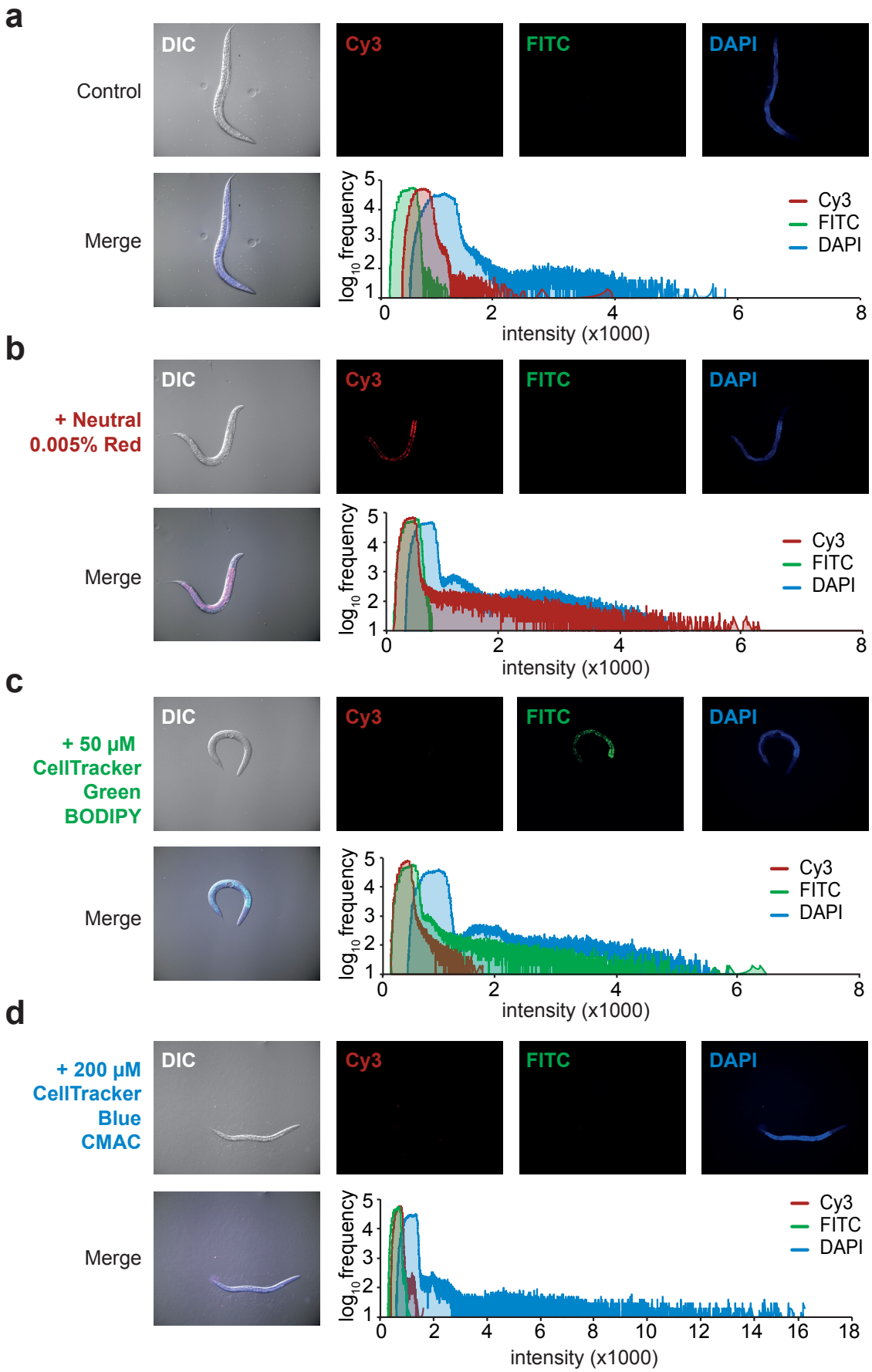

Supplementary Figure 4 | Vital dye staining of *Caenorhabditis elegans*.
a-d, Same as Supplementary Figure 2, but with *C. elegans*.

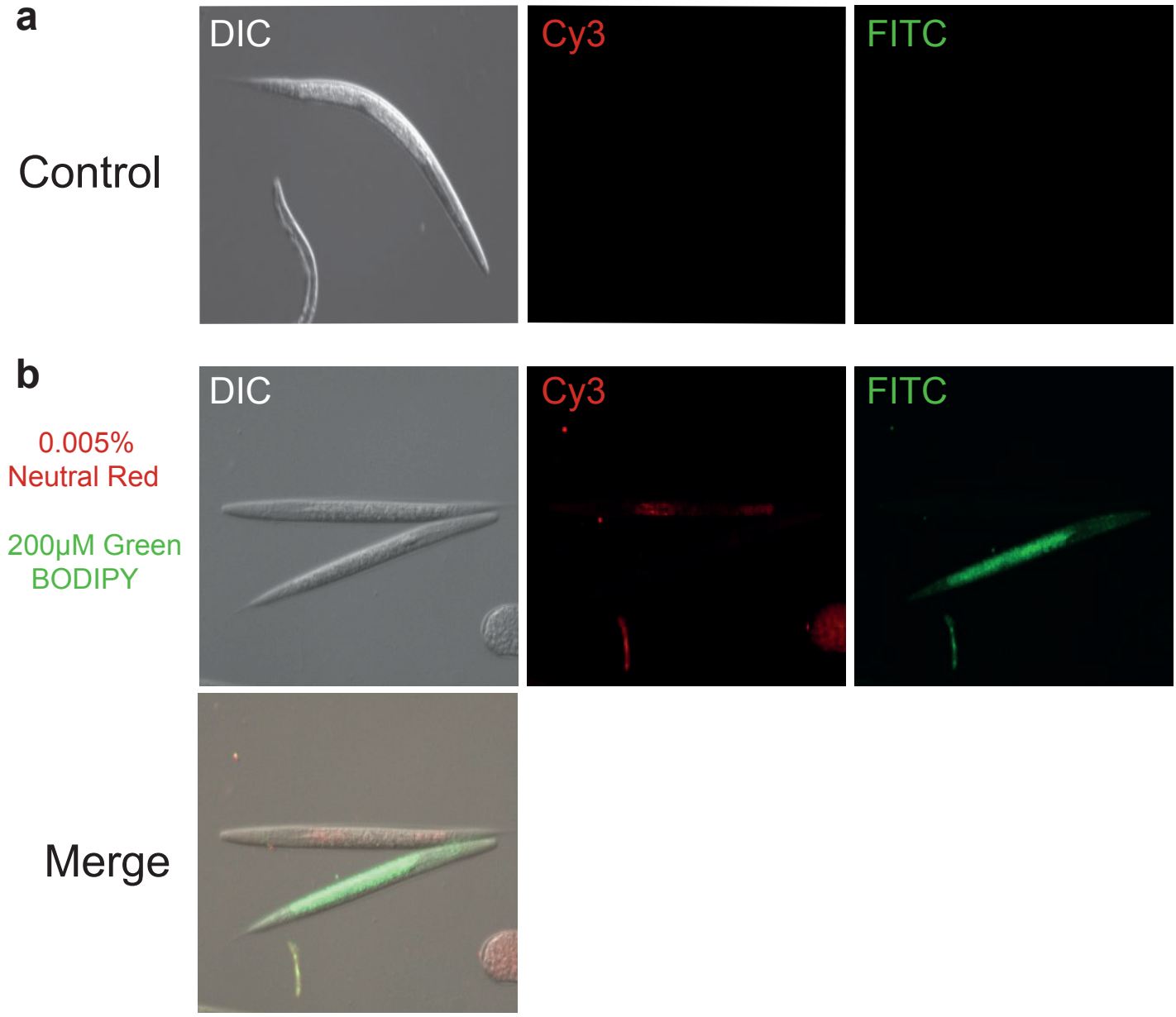

Supplementary Figure 5 | Vital dye staining of Pristionchus pacificus dauers. a, Control *P. pacificus* dauer imaged with DIC, Cy3, and FITC filters. **b**, Dauers stained with either 0.005% Neutral Red or 50 mM CellTracker Green Bodipy and imaged immediately after staining with DIC, Cy3, and FITC filters and merged with DIC. Images were taken using Zeiss Axio Imager 2 with an Axiocam 506 mono, processed using Zen-2pro software, and enhanced in ImageJ, all images with a display value minimum of 21 and maximum of 117.

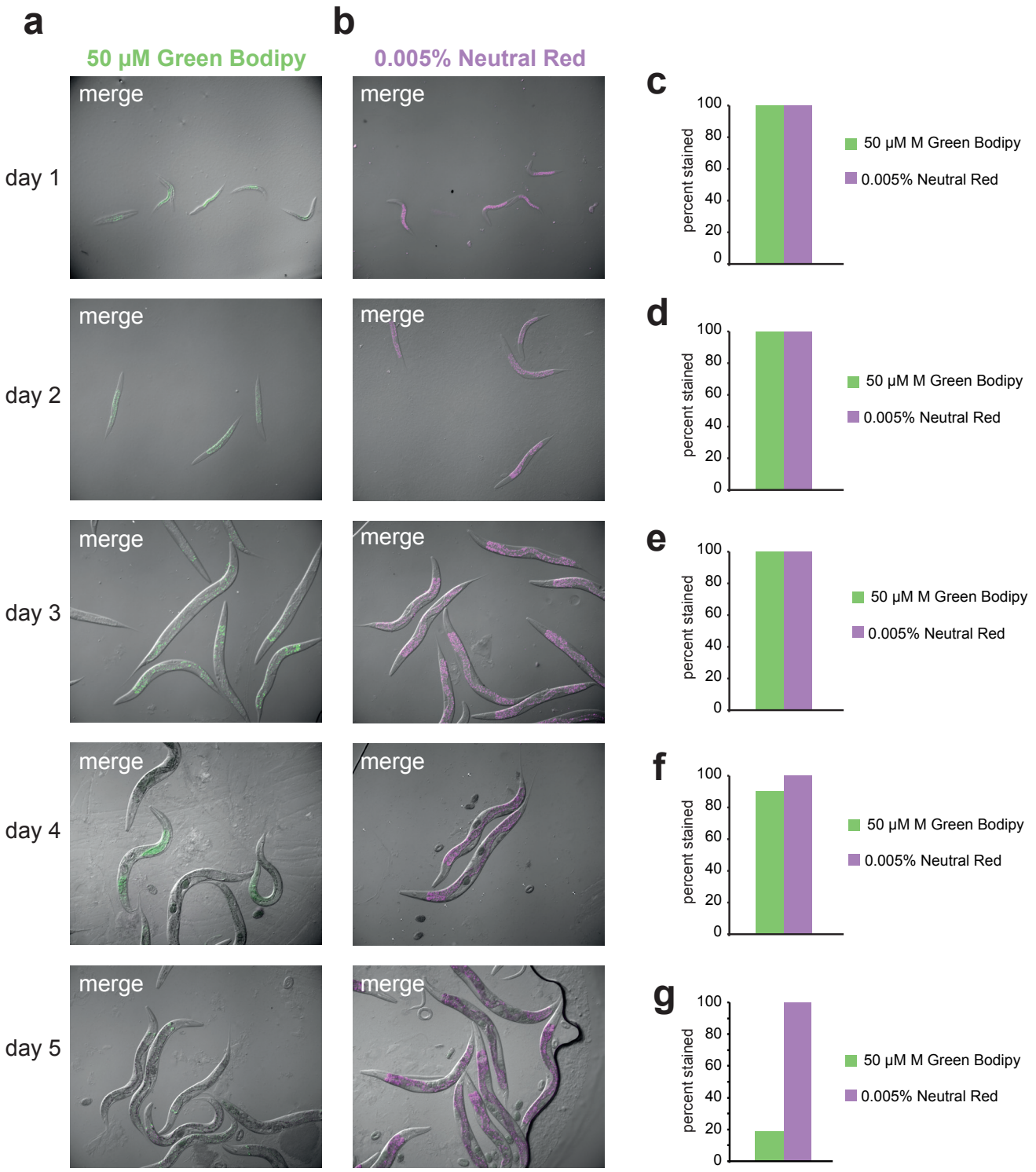

Supplementary Figure 6 | Vital dye staining lasts several days through development. **a**, 50 mM Cell Tracker Green Bodipy (GB) and **b**, 0.005% Neutral Red (NR)-stained J2s were imaged every day for five days. Percent of individuals retaining the dyes is shown in panels **c-g** for each day. Both stains are seen in all organisms for three days; NR persists for at least five, while the number of stained GB drops on day four. All images are merged with DIC, n=31 GB, 63 NR day 1, 68 GB, 56 NR day 2, 50 GB, 50 NR day 3, 50 GB, 50 NR day 4, 50 GB, 50 NR day 5.

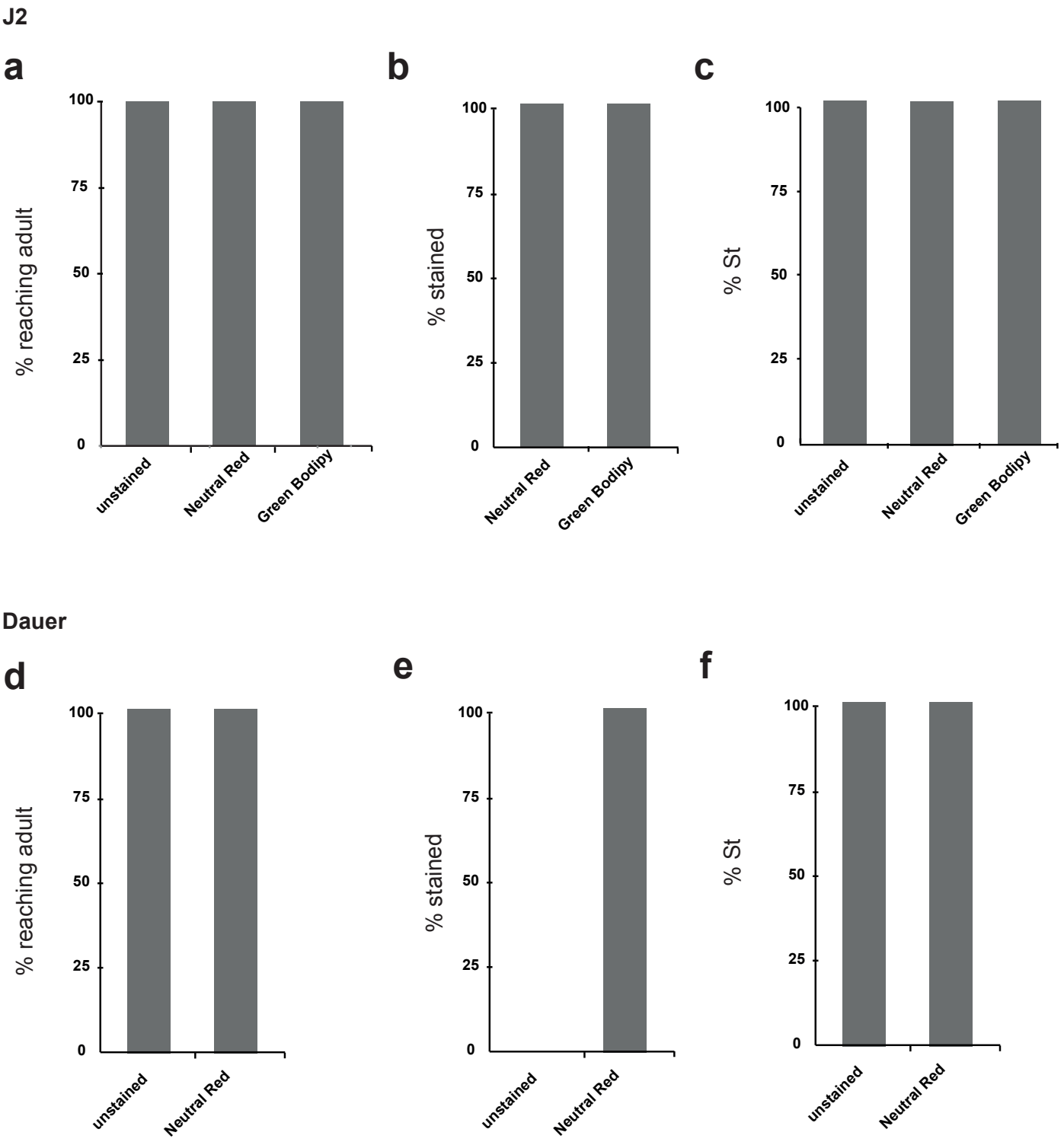

Supplementary Figure 7 | Vital dye staining does not affect *P. pacificus* mouth form or development. **a**, Neutral Red and CellTracker Green Bodipy-stained J2s reach adulthood at the same rate as unstained J2s (3 days). **b**, All of the J2s stained retain the dye in adulthood in the intestine. **c**, Neither dye affects mouth form; both unstained and stained worms remain 100% St (n=30). **d-f**, Same as for **a-c**, except with dauers instead of J2s, and only with Neutral Red.

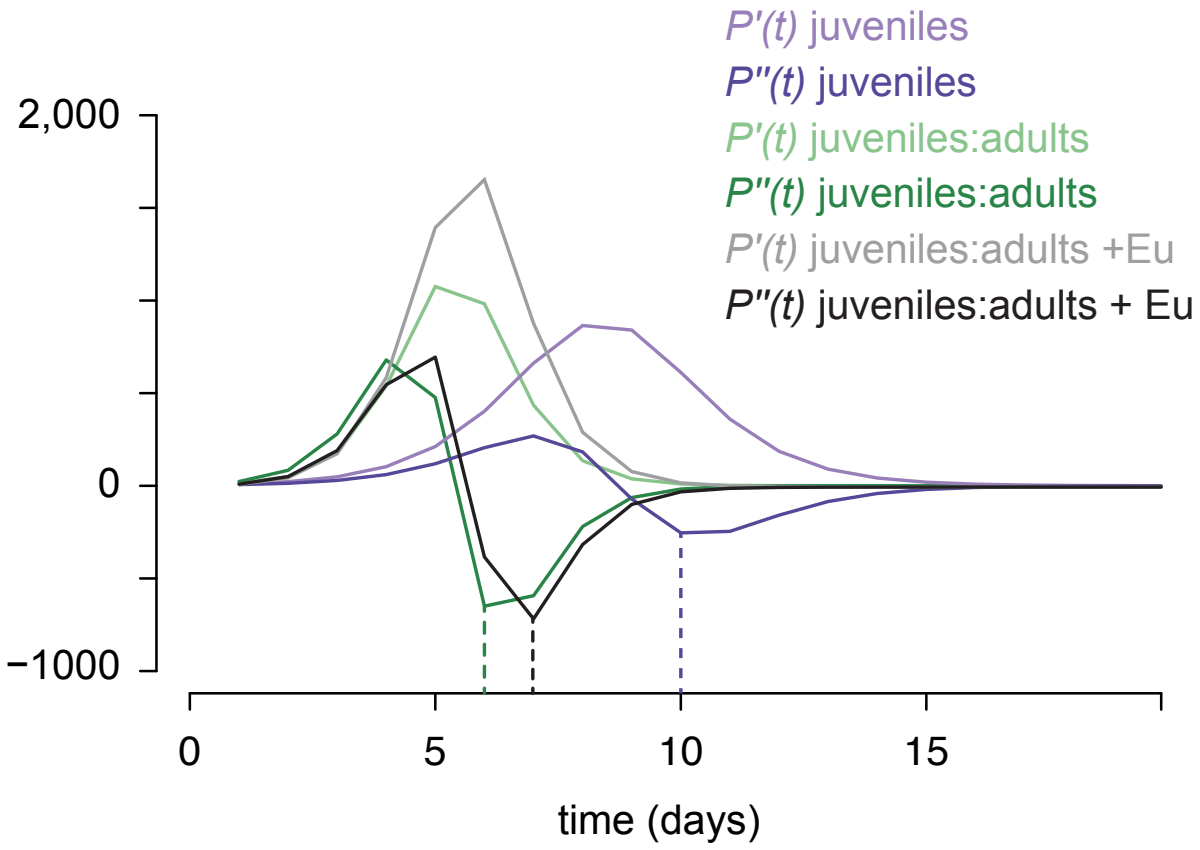

Supplementary Figure 8 | Second-derivative minima yield effective carrying capacity 'K'. First and second derivatives were calculated and then plotted in R. The times (days) at second derivitive minima were used to assess when each population approaches the effective carrying capacity 'K', which = six for juvenile:adult, ten for juvenile only, and seven for adult:juvenile populations that are modelled with a 1.5-fold increase in K as a result of Eu mouth forms.